Chapter 1: INTRODUCTION

Nucleation is the process with which the formation of new phases begins and is thus widely spread phenomenon in both nature and technology. Condensation and evaporation, crystal growth, deposition of thin films and overall crystallization are only a few of the processes in which nucleation plays a prominent role. Nucleation is nowadays believed to be involved in such apparently different phenomena as, for example, volcano eruption, electron condensation in solids, formation of black holes in the Universe, development of decompression sickness in deep-sea divers, irradiation-induced formation of voids in nuclear reactors, rupture of foam, membrane and emulsion bilayers, formation of electron-hole liquid in semiconductors, and in more widely fields, moreover it should not be a surprise if it proves that even the Big Bang was a nucleation phenomenon.

At present, nucleation is an established area of research and technology: in 1926, the first paper on the kinetics of nucleation was published by Volmer and Weber,[1] but already Gibbs in his thermodynamic works from the end of the nineteenth century obtained basic theoretical results in the area. Fundamentally, nucleation is a topic in the physics of the first-order phase transitions.

Homogeneous nucleation occurs when the clusters of the new phase are in contact only with the old phase and with no other phases and/or molecular species. Nucleation of droplets in the bulk of ideally pure supersaturated vapors is a classical example of homogeneous nucleation. On the other hand, heterogeneous nucleation, in which the already-existent of other phases and/or molecular species, is much widespread in both nature and technology, yet understanding the homogeneous nucleation has an importance as fundamentals of phase transitions.

Supersaturated vapor generates various sizes of nuclei. If the generated nucleus was smaller than a certain size, the nucleus should collapse and disappear. On the other hand, the larger nucleus should grow up to a liquid droplet. The size and the nucleation free energy of the critical nucleus play important roles for growth of the liquid droplet.

Experimental and theoretical studies for the homogeneous nucleation have been much widely carried out especially about the critical nucleus. In below, we introduce some discussions for the homogeneous nucleation and phase transition on the equilibrium theory and the kinetics.

1.1. Equilibrium Theory of Phase Transition[I]

Usually, the matters show among three phases; vapor, liquid, or solid. In the vapor phase, molecules scatter in the system. On the contrary, the solid phase molecules connect together regularly and do not move much. The liquid phase is an intermediate state of the vapor phase and the solid phase. In comparison between the vapor phase and the solid phase, internal energy of the latter is lower than one of the former because the solid phase has the intermolecular connection strongly than the other. On the other hand, entropy of the vapor phase is larger than one of the solid phase because the molecular configuration of the former is more disorderly than the other. The balance between the inclinations of internal energy and entropy, they are contrary each other, decides which phase is shown at given temperature and pressure: that is to say, the internal energy inclines to be lower and the entropy to be larger, which is modeled in Fig. 1.1. The free energy expresses the competition of the internal energy and the entropy as:

$$A = U - TS, \tag{1.1}$$

$$G = H - TS = U + PV - TS. \tag{1.2}$$

Equation 1.1 indicates the Helmholtz free energy A that defines correctly a most stable state of the system under given condition of (N,V,T), and eq. 1.2 Gibbs free energy G under (N,T,P). Here, the symbols U, T, S, H, P, V, and N are internal energy, temperature, entropy, enthalpy, volume, and the number of molecules of the system, respectively. The system changes spontaneously toward a state that obtain the lowest free energy. In the case of the Helmholtz free energy, when the temperature approaches to zero, the free energy is almost occupied by the contribution of the internal energy, therefore a state of the lowest free energy corresponds to one of the lowest internal energy, and the system shows the solid phase in which the molecules are connected together regularly. On the contrary, when the temperature rises, the entropy term contributes in remarkable; therefore a state of the lowest

free energy is given by one of the largest entropy. Accordingly, the system inclines the disorder configuration and the solid phase transits toward the liquid phase and the vapor phase. Similar discussions can be roughly adopted for the Gibbs free energy.

At the solid-liquid, liquid-vapor, or solid-vapor phase transition temperature, the two phases can coexist stably irrespective of which composition. That is to say, e.g., on the liquid-vapor coexistence state at the phase transition temperature T_t, even if the dN molecules changed from the liquid to the vapor or conversely from the vapor to the liquid, the total free energy of the system $G_{\text{total}} = G_{\text{liquid}} + G_{\text{vapor}}$ is constant at the minimum. Accordingly, at the T_t, the free energy change per molecule of the liquid phase should be equal to the one of the vapor phase as:

$$\mu_{\text{liquid}}(N, T_t, P) = \mu_{\text{vapor}}(N, T_t, P),$$
$$\mu_{\text{liquid}} = \left(\frac{\partial G_{\text{liquid}}}{\partial N}\right)_{T_t, P}, \quad \mu_{\text{vapor}} = \left(\frac{\partial G_{\text{vapor}}}{\partial N}\right)_{T_t, P}. \tag{1.3}$$

The symbol μ indicates chemical potential; that can be assumed as the free energy per molecule in the bulk phase. The chemical potentials of the each phase decide the direction of the phase transition by which magnitude, and indicate driving force of the phase transition by the difference between two phases $\Delta\mu$. For example, in the supercooled (supersaturated) vapor, the chemical potential of the vapor phase μ_{vapor} is larger than the one of the liquid phase μ_{liquid}, then the system inclines to transit toward the liquid phase, and the driving force of the phase transition is larger when the $\Delta\mu = \mu_{\text{vapor}} - \mu_{\text{liquid}}$ is larger.

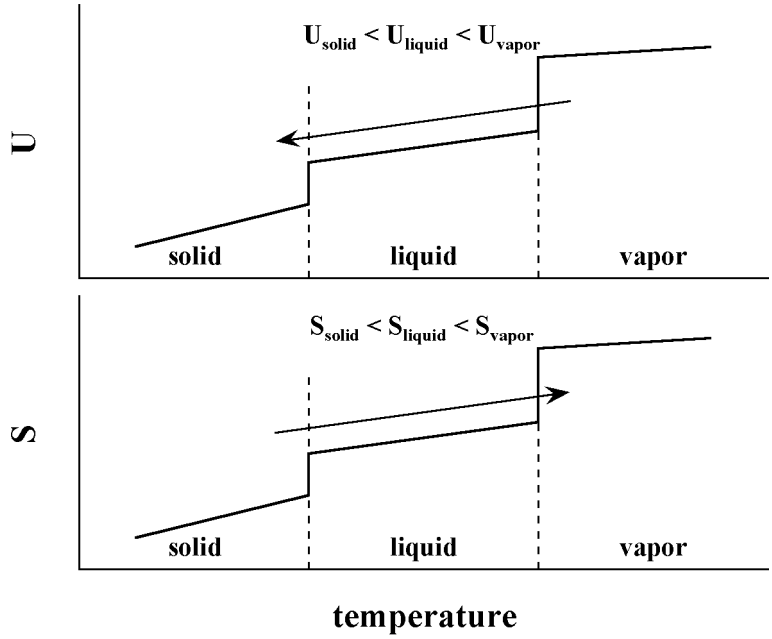

Fig. 1.1. Summary of the inclinations of internal energy and entropy. The arrows indicate the direction of the spontaneous change; the internal energy inclines to decrease, while the entropy to increase. Free energy negotiates the both and defines the most stable state by which minimum value.

1.2. Kinetics of the Homogeneous Nucleation[2,I]

According to the phase equilibrium theory discussed in the previous section, when the system is superheated or supercooled, the nuclei appear and grow immediately in the unstable phase, and the system ought to transfer toward the more stable phase. However, a metastable phase, a few superheated or supercooled systems, exists actually in which the nucleation and the phase transition do not occur. While, if the superheating or the supercooling ratio is above the certain criticality, the nucleation and the phase transition are observed. Such phenomenon is understood with kinetics of the nucleus growth.

1.2.1. Gibbs-Thomson's formula for the equilibrium pressure of the cluster

In the supersaturated vapor, the molecules collide each other and the nuclei grow up orderly as a monomer, dimer, trimer, tetramer... and larger cluster. In opposite, the going away of the molecule(s) from the cluster also occurs simultaneously. The nucleation rate J is expressed as the difference between the growth rate J_{cond} and the decay rate J_{evap}:

$$J = J_{\mathrm{cond}} - J_{\mathrm{evap}}. \tag{1.4}$$

Here, we consider about the nucleation rate in comparison with the kinetics of the bulk liquid-vapor equilibrium system.

The number of the vapor phase molecules that enter into the liquid phase per unit time per unit area, j_{in}, is described from the kinetics of vapor molecules:

$$j_{\mathrm{in}} = \frac{P}{\sqrt{2\pi mkT}}, \tag{1.5}$$

where m is mass of the molecule, k is the Boltzmann constant, and P is the system pressure. When the entered vapor molecules can be assumed to condense immediately into the liquid phase, the j_{in} can be regarded as the frequency of the condensation per unit area j_{cond}. In the liquid-vapor equilibrium system, the j_{cond} at the equilibrium pressure P_e equals to the frequency of the evaporation per unit time per unit area, j_{evap}, as

$$j_{\mathrm{evap}} = j_{\mathrm{cond}} = \frac{P_e}{\sqrt{2\pi mkT}}. \tag{1.6}$$

This corresponds to the equilibrium theory in which the chemical potentials of the both phases are identical if the system is in equilibrium as $\mu_{\mathrm{liquid}} = \mu_{\mathrm{vapor}}$.

On the other hand, in the case of the small-size cluster in the (supersaturated) vapor

phase, the contribution of the surface excess energy becomes remarkable because the ratio of the surface area against the volume of the cluster becomes larger, while the j_{evap} gets a dependence on the radius of cluster r; where the cluster is assumed as spherical-shape for easy consideration. The evaporation frequency of the cluster is larger than the one of the bulk liquid phase as

$$j_{evap}(r) > j_{evap}(\infty) = j_{cond} = \frac{P_e}{\sqrt{2\pi mkT}}. \tag{1.7}$$

Here, $j_{evap}(r)$ is the decay frequency of the cluster that depends on r, while $j_{evap}(\infty)$ is the one of the bulk liquid that can be regarded as $r = \infty$, because the surface is a plane. When the system pressure rises as far as obtain an identical decay-growth frequency,

$$j_{evap}(r) = j_{cond} = \frac{P(r)}{\sqrt{2\pi mkT}}, \tag{1.8}$$

the cluster equilibrates in the supersaturated vapor phase. The symbol $P(r)$ is the pressure of the supersaturated vapor phase that equilibrates with the cluster with the radius of r. Relation between the $P(r)$ and P_e is given as the Gibbs-Thomson's formula:

$$\ln\frac{P(r)}{P_e} = \frac{2\gamma}{\rho_c kTr}, \tag{1.9}$$

where ρ_c is the number density of the cluster and γ the density of the surface excess energy per unit area. If the system pressure is more than the equilibrium pressure of the bulk phases while less than the one of the small-size cluster, $P(r) > P > P_e$, the cluster decays as soon as which nucleation and the vapor preserves as the supersaturated phase. In other words, $P(r)/P_e$ becomes larger when the r becomes smaller, then the $P(r)$ is more than the system pressure, and there is strong probability that the cluster should decay without growing. On the other hand, the larger cluster which $P(r)$ is less then the system pressure should grow probably. Between both the sizes, the cluster with a certain radius of r^* obtains an identical pressure as $P(r^*) = P$, and equilibrates in the vapor phase. The r^* is termed as the critical radius, and the cluster with the radius of r^* as the critical nucleus. In the spontaneous formation of the various sizes of nuclei due to density fluctuation of the supersaturated vapor phase, the formation frequency of the cluster with the radius of $r > r^*$ per unit volume per unit time relates the nucleation rate J. The nucleation rate is interested in which dependence on the supersaturation ratio. The summary of the Gibbs-Thomson's formula is shown in Fig. 1.2, and the details are discussed in Appendix A.

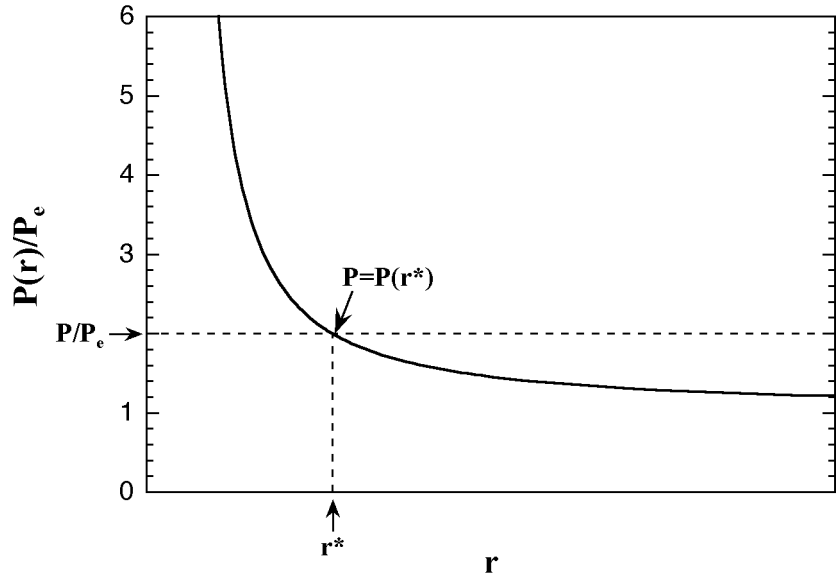

Fig. 1.2. The relation of the equilibrium pressure of the cluster with the radius of r and the one of the bulk vapor phase derived by the Gibbs-Thomson's formula. If the radius of cluster is a critical value r^*, the equilibrium pressure of the cluster is equivalent to the system pressure; the critical radius is given as $r^* = 2\gamma/\rho_c kT\ln(P/P_e)$, from eq. 1.9. The broken lines show a case of $P = 2P_e$.

1.2.2. Classical nucleation theory

In this section, we consider about the free energy change of the system accompanying the homogeneous nucleation. The classical nucleation theory considers the nucleation free energy ΔG as

$$\Delta G = \gamma A_s + \Delta g V. \tag{1.10}$$

Here, the first term indicates the surface contribution; γ is surface excess energy per unit area and A_s surface area of the cluster. While the second term is the bulk contribution; Δg is free energy change per unit volume between the bulk liquid phase and bulk the vapor phase, and V volume of the cluster. When the shape of cluster is assumed as spherical, A_s and V are expressed by the radius of the cluster r as $A_s = 4\pi r^2$ and $V = (4/3)\pi r^3$. The free energy change Δg is obtained as $\Delta g = -\rho_c kT \ln S$ from assumption of the vapor phase as an ideal gas, where ρ_c is density of the cluster and S supersaturation ratio. Such relations rearrange the eq. 1.10 as

$$\Delta G = 4\pi r^2 \gamma - \frac{4}{3}\pi r^3 \rho_c kT \ln S. \tag{1.11}$$

The radius r^* and the free energy ΔG^* of the critical nucleus are obtained as

$$r^* = \frac{2\gamma}{\rho_c kT \ln S}, \tag{1.12}$$

$$\Delta G^* = \frac{16\pi\gamma^3}{3(\rho_c kT \ln S)^2}. \tag{1.13}$$

The supersaturation ratio is expressed as $S = (P/P_e)$, where P and P_e are the pressures of the system and the equilibrated vapor phase. Accordingly, the expression of the critical radius of eq. 1.12, corresponds to the Gibbs-Thomson's formula shown in eq. 1.9. The r^* is in inverse proportion to the $\ln S$, therefore the larger supersaturation makes the r^* smaller.

Equation 1.11 is rearranged as a function of the number of cluster molecules by the relation of $N = \rho_c V$:

$$\Delta G = 4\pi\gamma\left(\frac{3N}{4\pi\rho_c}\right)^{2/3} - NkT \ln S, \tag{1.14}$$

and the size of the critical nucleus N^* is obtained as

$$N^* = \frac{32\pi\gamma^3}{3\rho_c^2 (kT \ln S)^3}. \tag{1.15}$$

Figure 1.3 shows the nucleation free energy ΔG from the classical theory.

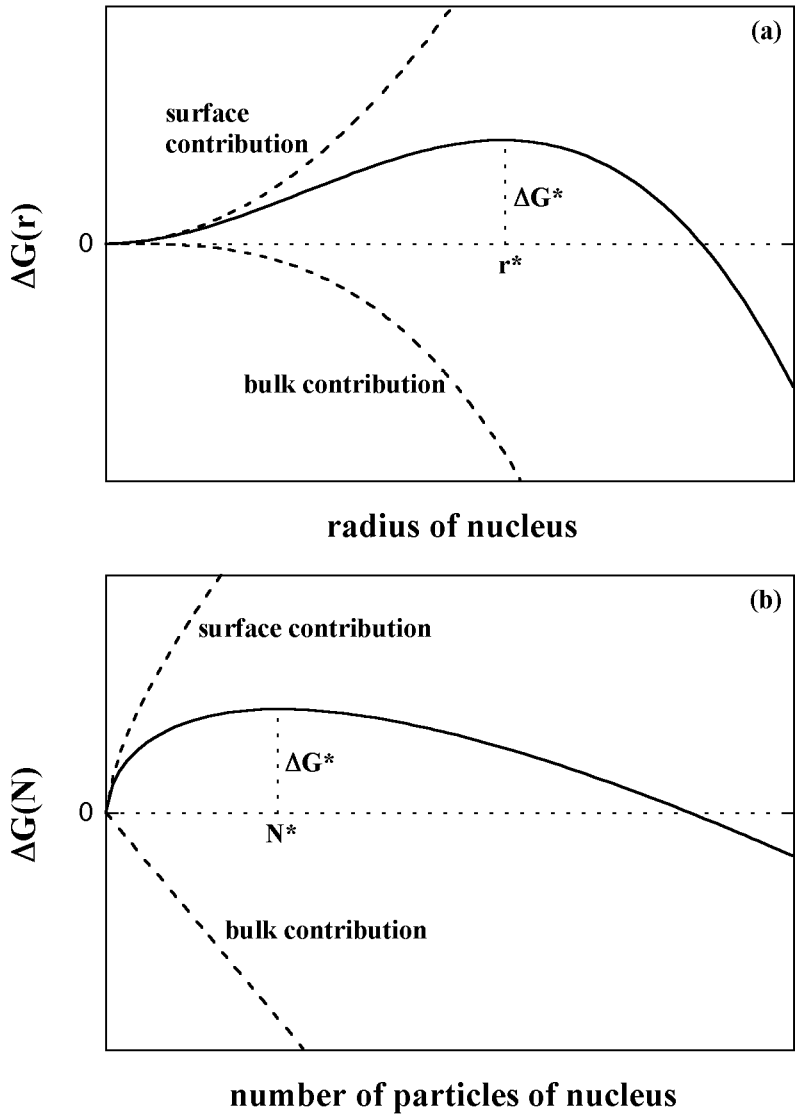

Fig. 1.3. Nucleation free energy ΔG as a function of (a) the cluster radius r and (b) the number of cluster molecules N predicted by the classical nucleation theory. The classical nucleation theory explains the ΔG as the sum of the surface contribution and the bulk contribution. Due to density fluctuation in the supersaturated vapor phase, if the generated cluster grows larger than the critical nucleus, the cluster should grow to macroscopic liquid droplet.

1.2.3. Nucleation rate[1]

In the process of the condensation/evaporation of molecules, when the size of the nucleus grows up larger than the critical size, the nucleus should grow up to the macroscopic cluster. Accordingly, the formation rate of the critical nucleus rules over the growth of the macroscopic cluster and the phase transition.

The density of the critical nuclei that are generated in the density fluctuation of the supersaturated system, q_r*, is expressed as a function of the free energy of the critical nucleus ΔG*:

$$q_r^* = q_{\mathrm{mono}} \exp \frac{-\Delta G^*}{kT}, \tag{1.16}$$

where q_{mono} is a density of the monomers in the supersaturated system. Moreover, when the frequency of the entering molecules into the critical nucleus is considered as ν_+, the nucleation rate J of the critical nucleus or the larger cluster is given as the product of the q_r* and the ν_+:

$$J = \nu_+ q_{\mathrm{mono}} \exp \frac{-\Delta G}{kT}. \tag{1.17}$$

In the case of the supersaturated vapor phase, the ν_+ equals to the product of the number of vapor molecules that enter into the nucleus (j_{in} in eq. 1.5) and the surface area of the critical nucleus. If the shape of the nucleus is spherical, the ν_+ is expressed as

$$\nu_+ = 4\pi r^{*2} \frac{P}{\sqrt{2\pi mkT}}. \tag{1.18}$$

As in eqs. 1.12 and 1.13, both the r* and the ΔG* are in inverse proportion to (the square of) the supersaturation ratio. Therefore, when the supersaturation ratio becomes larger, both the r* and the ΔG* become smaller, besides the J becomes smaller; the formation and the growth of the cluster becomes to be observed frequently. On the contrary, in a few-supersaturated system, since the nucleation rate becomes much larger, the cluster formation and the phase transition are not observed.

1.3. Purpose of This Study

The studies for the homogeneous nucleation with computer simulations have been widely performed. Giving the studies of recent years, Yasuoka and Matsumoto carried out large-system ensemble molecular dynamics (MD) simulations and estimated the size of critical nucleus and the free energy of nucleation from the cluster size distribution.[2-4] Oh and Zeng reported cluster size dependence of the nucleation energy by constrained Monte Carlo (MC) simulations in which applied upper limit of the cluster size.[5] They also performed small-system grand canonical ensemble MC method in which the cluster-vapor interaction is effectively taken into account.[6] Wolde and Frenkel obtained the nucleation energy by umbrella sampling.[7] Kusaka and Oxtoby suggested an approach to cluster simulation without a cluster criterion that is determination particle by particle whether it belongs to cluster or vapor phase for instantaneous configuration.[8]

The previous computational works performed on some particular states, then that do not predict the nucleation free energy on a wide range of the temperature and the pressure. In this work, we suggest a simple model and a method for the purpose of obtaining the free energy of the homogeneous nucleation by using the canonical MC simulations. In which, we assumed a technique for direct estimation of the free energy of the system, and we obtained the nucleation free energy as difference between the free energies of the cluster and the supersaturated vapor phase. Moreover, we approximated an equation of state (EOS) for the Helmholtz free energy of the nucleation from the MC results. We performed the two series of MC simulations; under a fixed volume per particles and various volumes per particle. In the former, we estimated the EOS as a function of the number of particles and temperature, while in the latter, we included the volume dependence toward the EOS. On the basis of the EOS in canonical ensemble, we rearranged the EOS to estimate Gibbs free energy of the nucleation as a function of the number of particle, the temperature, and the pressure.

Chapter 2: SUMMARY OF MONTE CARLO SIMULATION

2.1. Lennard-Jones Potential Function[9,II]

We applied the Lennard-Jones (LJ) 12-6 type potential function

$$\phi_{LJ}(r_{ij}) = 4\varepsilon\left\{\left(\frac{\sigma}{r}\right)^{12} - \left(\frac{\sigma}{r}\right)^{6}\right\}, \tag{2.1}$$

for the target particle. The LJ function describes the interaction between two particles as a simple function of which center-center distance, and has been widely used as a function that indicates the intermolecular interaction of monatomic molecules, simplified polyatomic molecules or groups, moreover the intramolecular interaction of the atoms or groups in polyatomic molecules. The sixth power term indicates an attractive part of the interaction, and the twelfth power term indicates a repulsive part. The attractive term is based on the dispersion force of the van der Waals crystal that is in inverse proportion to the sixth power of the intermolecular distance. On the other hand, the repulsive term, a integer among 9 to 15 is chosen as the number of power, yet the twelfth power has been widely used because the easily handling of the equation and the polarization inductive effect that is based on the secondary perturbation theory of the quantum mechanics. While such function, the combination of the *m*-th power of repulsive term and *n*-th power of attractive term, is commonly termed as the LJ *m*-*n* type potential function. The symbols ε and σ are the LJ parameters that correspond to the strength of the interaction and the size of the particle. The parameters are assumed for the noble gases, that are neutral, non-polar, and spherical-shaped monatomic molecules: ε/k = 36.21 K and σ = 0.274 nm for neon with k being the Boltzmann constant, 119.8 K and 0.340 nm for argon, 163.0 K and 0.365 nm for krypton, 231.8 K and 0.398 nm for xenon.[10] In this study, we used the LJ parameters as the reduced units: ε for energy and σ for length; volume σ^3, temperature ε/k, pressure ε/σ^3, etc. Figure 2.1 shows the LJ potential function in the reduced units.

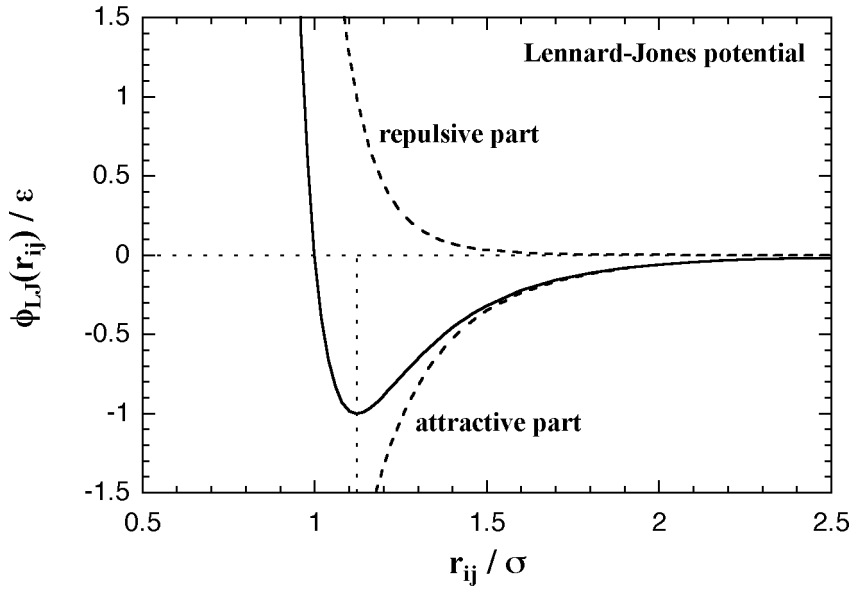

Fig. 2.1. Lennard-Jones 12-6 potential function. The function, given as eq. 2.1, is a combination of the repulsive part as the twelfth power term and the attractive part as the sixth power term. This 12-6 function obtains a minimum of $\phi_{LJ} = -\varepsilon$ at $r_0 = 2^{1/6}\,\sigma$, and the r_0 corresponds to radius of the particle.

2.2. Model of Homogeneous Nucleation

In this study we suggest a simple model to estimate the free energy of the homogeneous nucleation in the supersaturated LJ system. Figure 2.2 gives a summary of the model. In the upper figure, a conventional large-system model contains large number, that is at least several thousands, of target particles. The density corresponds to the supersaturated vapor, and according to circumstances, carrier gas particles are included in the system. During the MC/MD simulations, the small-size nuclei have generated and grown spontaneously in the system. On the other hand, in the lower figure, we focus a specific number of particles N, and put the N target particles and no carrier gas particles into the system. Here, the two extremes are supposed for the N-particle system: namely, cluster phase and monomer phase. The former is a state in which all particles of the system are connecting together as a N-particle cluster, and in the latter all particles are scattering as a supersaturated vapor phase. When the free energies of the cluster phase G_c and the monomer phase G_m are obtained independently, the free energy of the N-particle nucleation ΔG can be assumed as the difference of the latter from the former:

$$\Delta G = G_c - G_m. \tag{2.2}$$

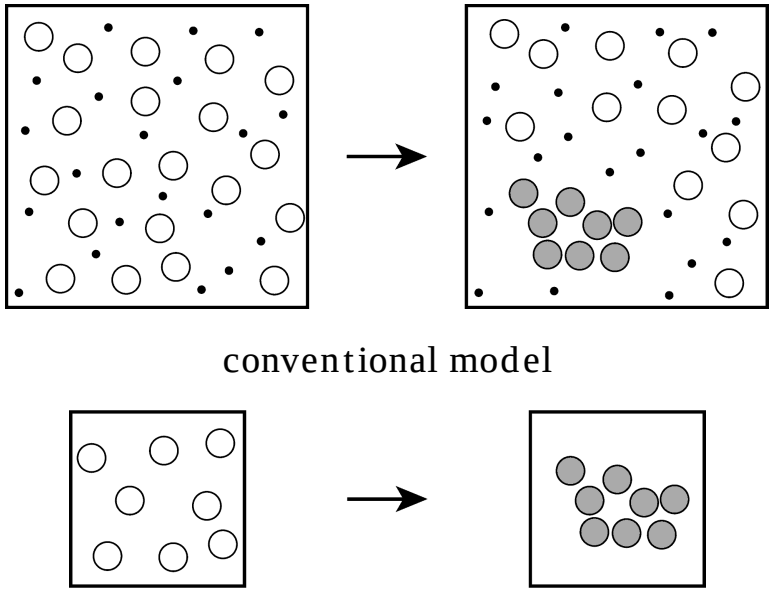

Fig. 2.2. The process of *N*-particle nucleation in the large system that includes the carrier gas particles is modeled as the nucleation of the whole particles in the *N*-particle system. The circles indicate the target gas particles, and the shadowed circles the nucleated particles. Though the dots indicate the carrier gas particles in the conventional model, it is not included in our model. Since the cluster phase requires that the all particles in the system consist a unity cluster, the surrounding of the cluster is a vacuum.

2.3. Monte Carlo Procedure

We explain below the detailed procedure of the MC simulations. The volume per particle V/N is chosen as the supersaturated vapor phase. Figure 2.3 shows phase diagram of LJ fluid on density-temperature plane that is based on the equation of state derived by Nicolas et al.[11] The number of particles N, for which we focused respective values, is set among 2 up to 80. The basic cell is cubic, that contains N target particles and no carrier gas particles, in which the periodic boundary conditions for all three dimensions are adopted. The cut-off distance of the LJ interaction is a half of cell width, and a correction term is adopted for contributions from more distant particles.

As we stated in the previous section, the cluster phase and the monomer phase should be simulated independently for the purpose of the free energy estimation. Then, we performed four stages of the MC calculations: namely, cluster stabilization process, phase transition calculation, cluster phase calculation, and monomer phase calculation. The first stage, the cluster stabilization, prepares an initial cluster for the phase transition and the cluster phase calculations. An initial configuration of this stage is chosen among distorted simple cubic, body-centered cubic, or face-centered cubic lattices by the number of particles. If the N particles do not fill the lattice, the defect(s) is (are) inserted into the lattice site(s). Starting with the initial lattice, the particles are stabilized as a cluster by the cooling MC calculation. From the initial temperature 0.20 ε/k, the system is cooled to 0.01 ε/k in 0.01 ε/k steps. We calculated at least 4 million MC steps severally for equilibration and statistics at each temperature; where we regarded one MC step into N trial movements. The stability and structure of the cluster are discussed in Appendix B. The second stage is the phase transition calculation. The stabilized cluster created in the first stage is heated up from 0.01 to 1.00 ε/k in 0.01 ε/k steps; where one million MC steps were calculated for equilibration and statistics at each temperature. The cluster decomposes to the monomer phase (the supersaturated vapor phase) at a certain temperature that depends on the number of particles. Thirdly, the cluster phase calculation also uses the stabilized cluster as an initial configuration and the system is heated up similarly to the second stage. However, the cluster decomposition, i.e., leaving of any particle from the N-particle cluster, is prohibited in this stage. We applied Stillinger's cluster criterion[12] for this purpose. According to the Stillinger's criterion, any two particles are connected if their center-center

distance is less than a threshold distance. After each MC movement, we examined the new configuration whether all particles of the system are mutually connected. If the new configuration was not considered as a unity cluster, it was rejected before the Metropolis judgment and was not counted as the number of the MC trial. We selected the threshold distance as 1.5 σ, that has been used and examined widely,[2,3,5] and corresponds to the first minimum of the pair correlation function of the cluster (or bulk liquid) phase. The pair correlation function of the phase transition calculation is shown in Fig. 2.4. The third stage obtains the superheated cluster phase above the phase transition temperature. Lastly, we performed the monomer phase calculation. Contrary to the cluster phase calculation, any connections should be refused in this stage. That is to say, all combinations of the center-center distances of the particles in the system should be longer than 1.5 σ. After each MC trials, if the new configuration had any connections, the trial was canceled. The initial lattice is similar to the cluster stabilization process, however all the interparticle distances are set to be longer than the threshold value as the monomer phase. Starting with initial temperature 1.00 ε/*k*, the system was cooled to 0.01 ε/*k* in 0.01 ε/*k* steps; where between 100 thousands to one million MC steps were calculated for equilibration and statistics severally at each temperature. Supercooled monomer phase is obtained in this stage. Figures 2.5-2.8 show sample snapshots of the stabilized cluster, the decomposed monomer phase in the phase transition calculation, the superheated cluster phase, and the supercooled monomer phase on 32-particle system.

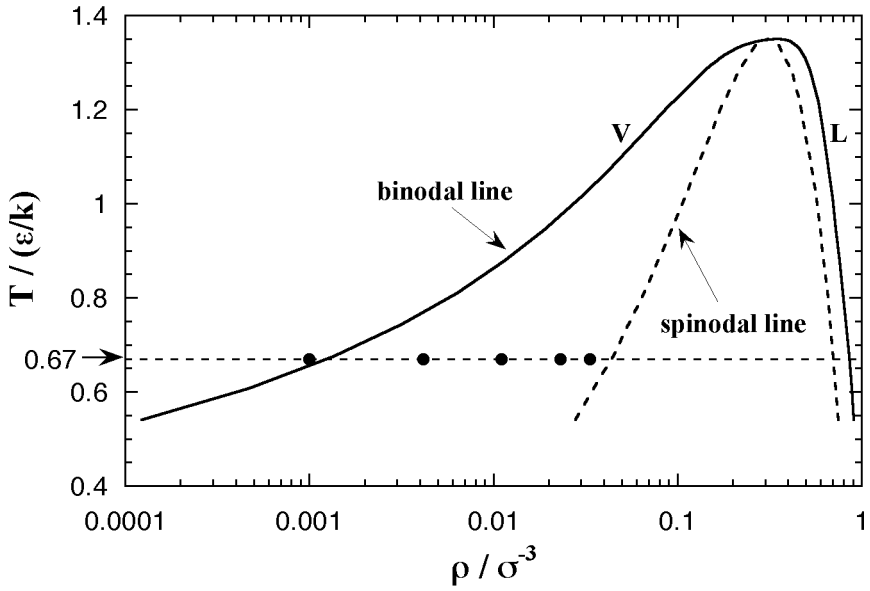

Fig. 2.3. Phase diagram of the Lennard-Jones fluid.[11] The solid line indicates the binodal (liquid-vapor coexistence) line, and the broken line indicates the spinodal (boundary of thermodynamically unstable region) line. The arrow indicates the near of triple point temperature of the LJ fluid, 0.67 ε/*k*, that we focused. The dots are the simulated densities (inverse of volumes per particle) in Chapters 3 and 4; at the focused temperature, the densities roughly exist in the metastable region between the binodal and spinodal lines.

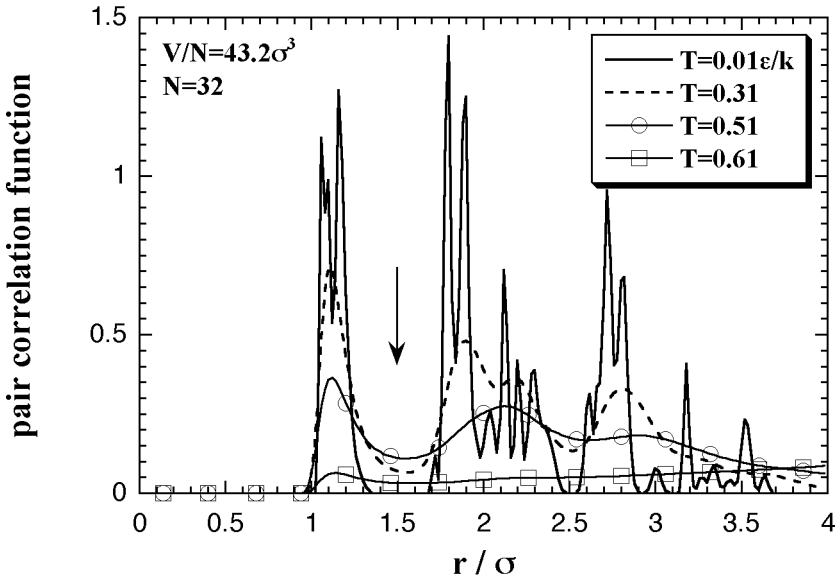

Fig. 2.4. Pair correlation function of the phase transition calculation on 32-particle system at several temperatures. Though the pair correlation function is usually normalized by random distribution, no normalization is performed in this figure. The arrow indicates the first minimum of the function, ca. 1.5 σ, it corresponds to the threshold distance of the Stillinger's cluster criterion. The peaks disappear between temperature 0.51 to 0.61 ε/*k*, therefore the cluster decomposition occurs during the temperature.

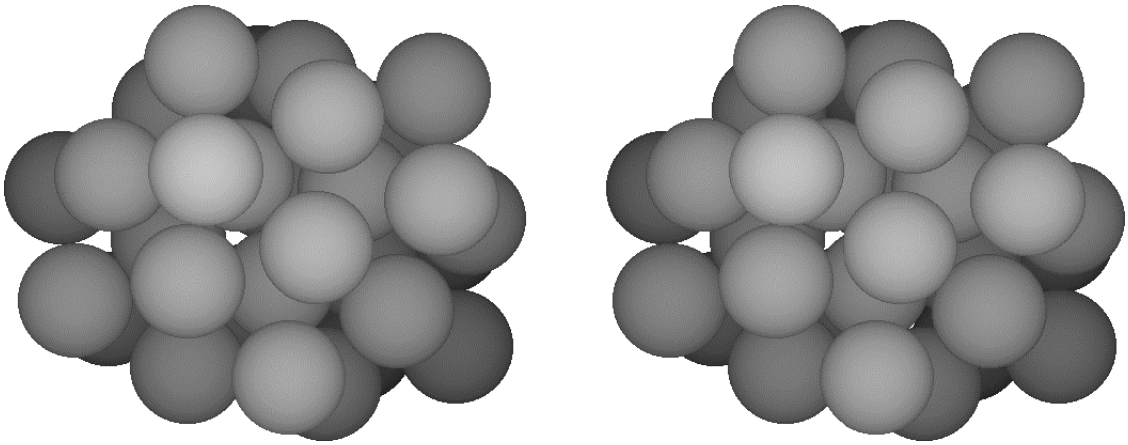

Fig. 2.5. Stereoscopic snapshot at the end of the cluster stabilization process; $N = 32$, $T = 0.01\ \varepsilon/k$, $V/N = 43.2\ \sigma^3$. The details of the stable structure of LJ cluster is discussed in Appendix B.

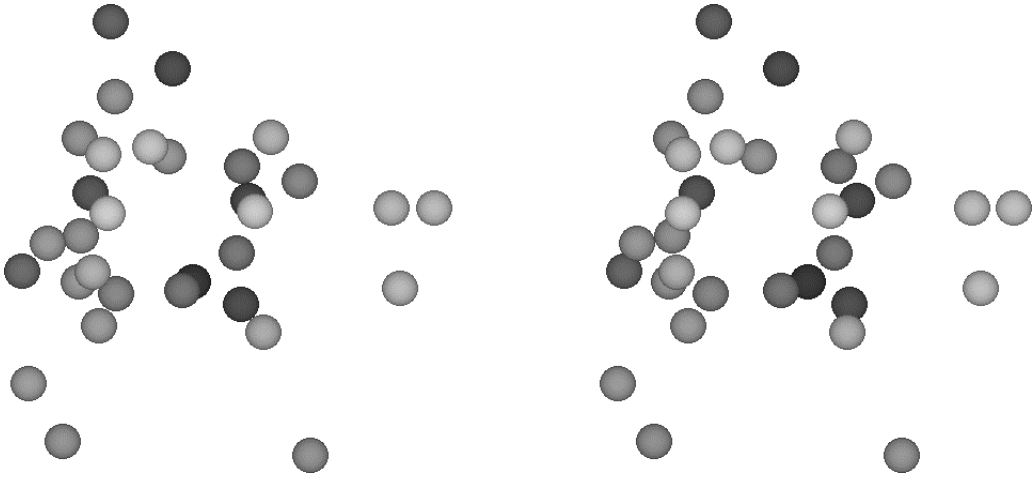

Fig. 2.6. Stereoscopic snapshot of the decomposed monomer phase at the end of the phase transition calculation; $N = 32$, $T = 1.00\ \varepsilon/k$, $V/N = 43.2\ \sigma^3$.

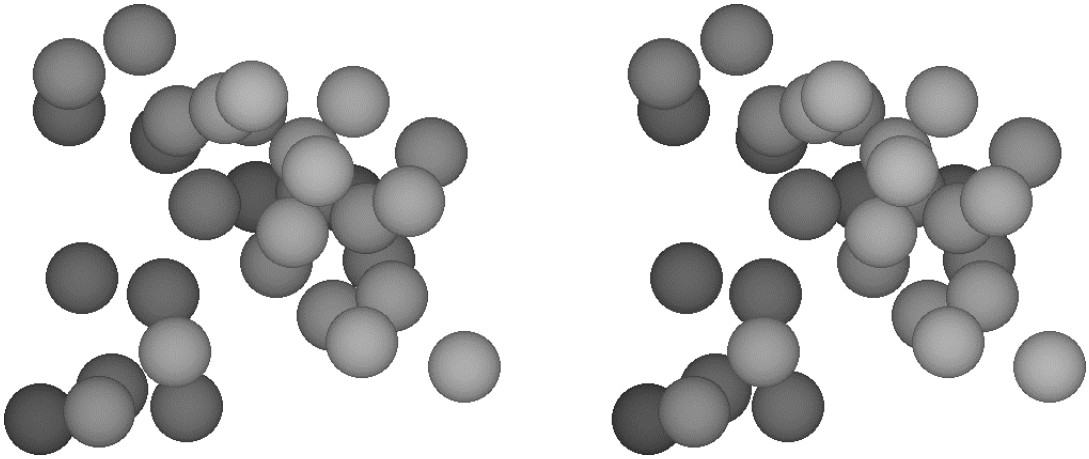

Fig. 2.7. Stereoscopic snapshot of the superheated cluster phase at the end of the cluster phase calculation; $N = 32$, $T = 1.00\ \varepsilon/k$, $V/N = 43.2\ \sigma^3$.

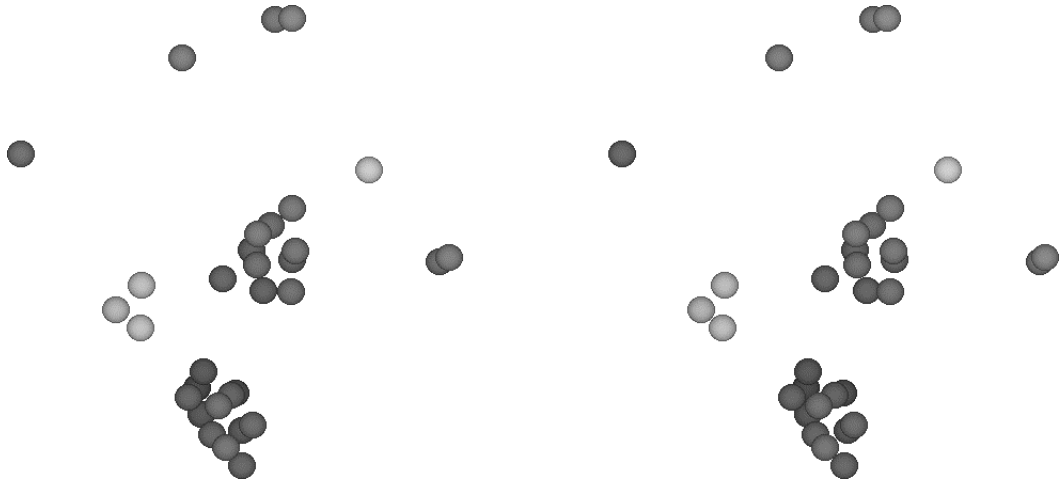

Fig. 2.8. Stereoscopic snapshot of the supercooled monomer phase at the end of the monomer phase calculation; $N = 32$, $T = 0.01\ \varepsilon/k$, $V/N = 43.2\ \sigma^3$.

2.4. Free Energy Estimation

An interaction term of Helmholtz free energy A^e under constant volume is estimated as

$$A^e = U^e - TS^e, \tag{2.3}$$

where U^e indicates an average value of interaction energy of the system, T temperature and S^e an interaction term of entropy. During the MC calculation, the U^e can be easily obtained as the sum of two-body interaction energies as

$$U^e(N,T,V) = \left\langle \sum_{(ij)} \phi_{LJ}(r_{ij}) \right\rangle_{NTV} . \tag{2.4}$$

However, there are some difficulties in obtaining the interaction entropy. We estimated the interaction entropy as follows:[9]

$$C^e(N,T,V) = \left(\frac{\partial U^e}{\partial T}\right)_{NV}, \quad \text{or} \tag{2.5}$$

$$C^e(N,T,V) = \frac{1}{kT^2}\left[\left\langle \left(\sum_{(ij)} \phi_{LJ}(r_{ij})\right)^2 \right\rangle_{NTV} - \left\langle \sum_{(ij)} \phi_{LJ}(r_{ij}) \right\rangle_{NTV}^2\right], \tag{2.6}$$

$$\begin{aligned} S^e(N,T,V) &= \int_{T_0}^{T} \frac{C^e(N,T,V)}{T}\, dT + S^e(T_0) \\ &= \sum_i \frac{C_i^e(N,T,V)}{T_i}\Delta T + S^e(T_0). \end{aligned} \tag{2.7}$$

We obtained an interaction term of the heat capacity as the numerical differentiation, eq. 2.5, or the fluctuation, eq. 2.6, of the interaction energy, besides we obtained the interaction entropy as the thermodynamic integration, eq. 2.7, of the heat capacity. Here, in eq. 2.7, each temperature interval of the thermodynamic integration ΔT is 0.01 ε/k, and the lower end of the calculated temperature T_0 is also 0.01 ε/k, thus

$$S^e(T_0) = \frac{C^e(T_0)}{T_0}\Delta T = C^e(T_0). \tag{2.8}$$

Accordingly, the interaction entropy obtained in this study is a relative value that has the same starting point as the heat capacity at $T_0 = 0.01\ \varepsilon/k$.

When the Helmholtz free energies of the cluster phase A_c^e and monomer phase A_m^e under constant volume are obtained independently, the free energy change of the nucleation ΔA is regarded as

$$\Delta A(N,T,V) = A_c^{\,e}(N,T,V) - A_m^{\,e}(N,T,V). \tag{2.9}$$

In eqs. 2.3-2.9, we neglected the ideal gas terms of internal energy, heat capacity, entropy, and Helmholtz free energy. However, if the volume is constant, the ideal gas terms are identical irrespective of the configuration of the system, and canceled by subtraction in eq. 2.9. Therefore, the neglect is adequate for the purpose of ΔA estimation.

On the other hand, Gibbs free energy is sum of the Helmholtz free energy and the product of the pressure P and the volume V:

$$G = A + PV. \tag{2.10}$$

The Gibbs free energy of the nucleation should be obtained under constant pressure as

$$\Delta G(N,T,P) = G_c(N,T,P) - G_m(N,T,P) = G_c(N,T,V_c) - G_m(N,T,V_m), \tag{2.11}$$

where V_c and V_m are volumes of the cluster phase and the monomer phase that present an identical pressure P. In this equation, the ideal gas terms of the each phase are not canceled because the ideal gas term of the Gibbs free energy depends on the volume. Accordingly, to obtain the ΔG on (N,T,P) domain, the ideal gas terms $G_c^{\,id}$ and $G_m^{\,id}$ should be taken into account as

$$\begin{aligned}\Delta G(N,T,P) = \\ \{G_c^{id}(N,T,V_c) + G_c^{e}(N,T,V_c)\} - \{G_m^{id}(N,T,V_m) + G_m^{e}(N,T,V_m)\}.\end{aligned} \tag{2.12}$$

Chapter 3: MONTE CARLO SIMULATIONS UNDER A FIXED VOLUME PER PARTICLE

3.1. Monte Carlo Results

First, we performed the MC simulations under a fixed volume per particle to estimate the EOS of the Helmholtz free energy of the homogeneous nucleation as a function of the number of particles and the temperature. The volume per particle $V/N = 43.2\ \sigma^3$. This value corresponds to supersaturated vapor phase (see Fig. 2.3) and recent MD simulations by Yasuoka and Matsumoto.[2,3] Here we explain and discuss about the results of the MC simulations.

Both the interaction energy and the interaction entropy increase in proportion to the number of particles in a sufficiently large system. Then, we mainly treat about the thermodynamic quantities as values per particle.

As an example of MC results, the thermodynamic properties of a 32-particle system are shown below. Figure 3.1 shows averaged interaction energy per particle versus temperature. In the phase transition calculation, the stabilized cluster decomposes to the monomer phase at a certain temperature that depends on the number of particles. The phase transition temperature is ca. $0.57\ \varepsilon/k$ in the 32-particle system. Though the equilibrated value of the decomposed monomer phase in the phase transition calculation should correspond to the value of the monomer phase calculation, they did not agree. As we stated above, the each interparticle distance is restricted to be longer than $1.5\ \sigma$ in the monomer phase calculation, yet the restriction is not applied in the phase transition calculation. From this difference of condition, it is conjectured that the equilibrated interaction energy of the two calculations would disagree. The monomer phase calculation gives an ideal vapor phase; however, we consider that the decomposed monomer phase in the phase transition system is more close to the real monomer phase. Accordingly, we corrected the curve of the monomer phase calculation to agree with the

equilibrated value of the decomposed monomer phase in the phase transition calculation. Moreover, this correction aims to create a relation between the cluster phase calculation and the monomer phase calculation.

Figure 3.2 shows the interaction term of heat capacity that is obtained from eqs. 2.5 or 2.6. In the figure, (a) the results of phase transition calculation, while (b) cluster and monomer phase calculations are each shown. On the phase transition calculation, the temperature that indicates the maximum heat capacity corresponds to the cluster-monomer phase transition temperature 0.57 ε/k.

The interaction entropy from the thermodynamic integration of eq. 2.7 is shown in Fig. 3.3. Here, the corrections for the interaction energy were also adopted for the curves of monomer phase calculation as the figure (b). In the figure (a), we confirmed the equality of the interaction entropy from the two ways of the heat capacity estimation (eqs. 2.5 and 2.6). Accordingly, we decided to adopt the numerical differentiation of the interaction energy, eq. 2.5, for the heat capacity estimation.

The interaction term of Helmholtz free energy is shown in Fig. 3.4. The intersection of the curves of the cluster phase and the monomer phase calculations indicates a phase transition temperature, it is 0.55 ε/k at the 32-particle system. The figure (b) is a magnification nears the phase transition temperature. On the phase transition calculation, the cluster decomposes gradually over some range of temperature that is centering around the phase transition temperature since the calculation was not adopted any restrictions on the configuration. Accordingly, a peak of the heat capacity on the phase transition calculation, 0.57 ε/k in the 32-particle system, does not always agree with the intersection of the curves of the monomer phase and the cluster phase calculations. The phase transition temperatures from the peak of the heat capacity and the intersection are compared in Fig. 3.5. There is not much different in both plots.

Lastly, the Helmholtz free energy of the nucleation ΔA, which is obtained as the difference between the free energies of the cluster phase and the monomer phase, is plotted versus the number of particles in Fig. 3.6. The figure (b) gives the Helmholtz free energy of the N-particle nucleation and the critical values of the nucleation, the size and the free energy, by which maximum.

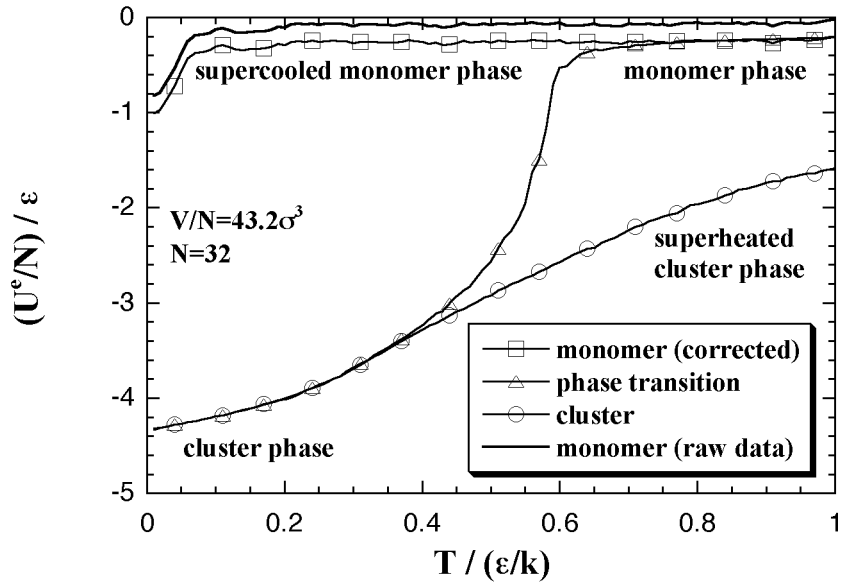

Fig. 3.1. The interaction energy per particle versus temperature plots on 32-particle system. On the phase transition calculation, the cluster decomposes to the monomer phase at $T \sim 0.57\ \varepsilon/k$. The curve of the monomer phase calculation (the broken curve) is corrected to agree with the equilibrated value of the decomposed monomer phase in the phase transition calculation.

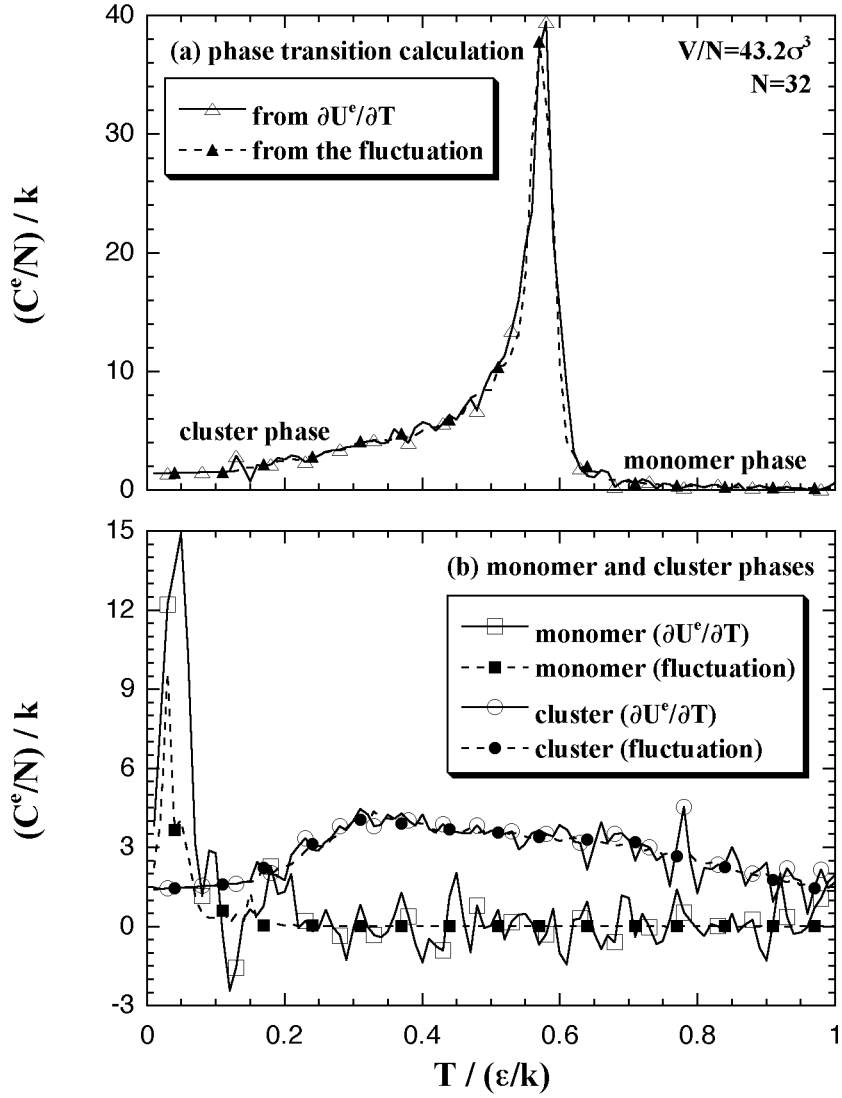

Fig. 3.2. The interaction term of heat capacity per particle versus temperature plots. The results of the phase transition calculation (a), the monomer phase and the cluster phase calculations (b) are shown. The solid curves are the values obtained from the differentiation of the interaction energy, while the broken curves are from the fluctuation.

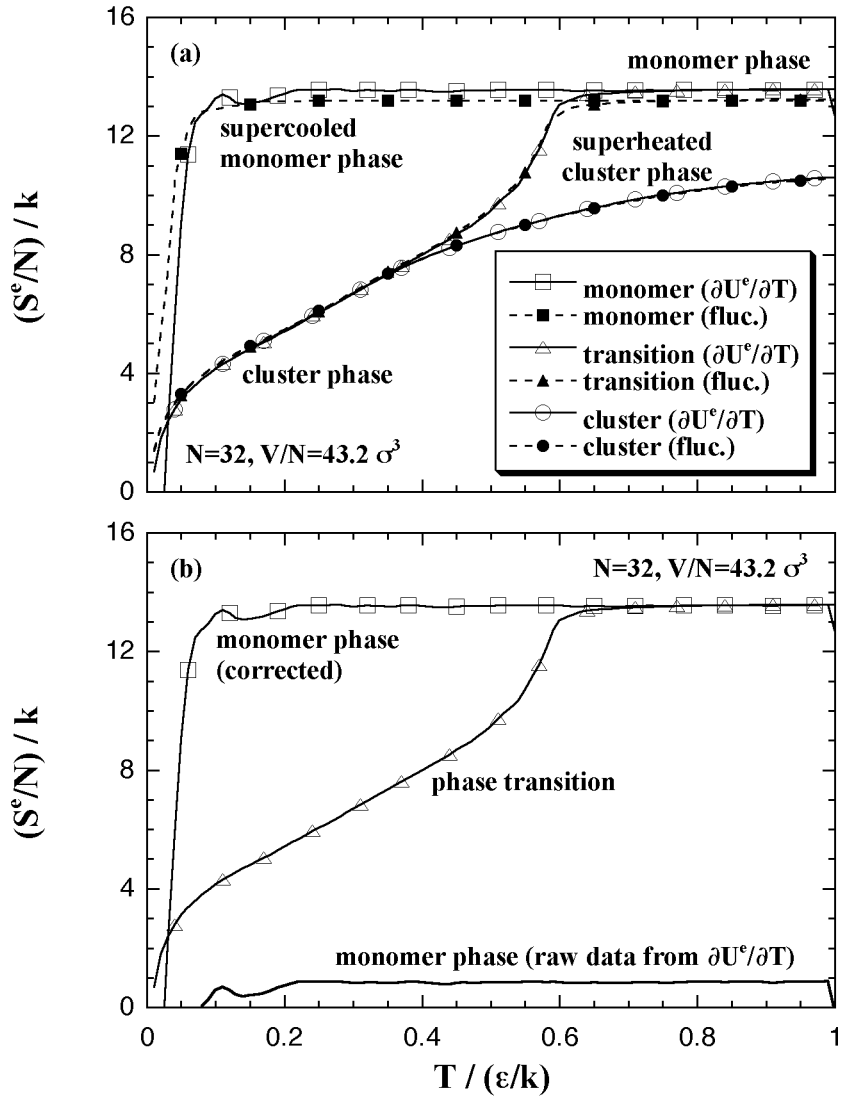

Fig. 3.3. The interaction entropy per particle versus temperature plots. In the figure (a), the curves from two ways of heat capacity estimation are nearly agreed. The curve of the monomer phase calculation is corrected to agree with the decomposed monomer phase in the phase transition calculation, as shown in the figure (b).

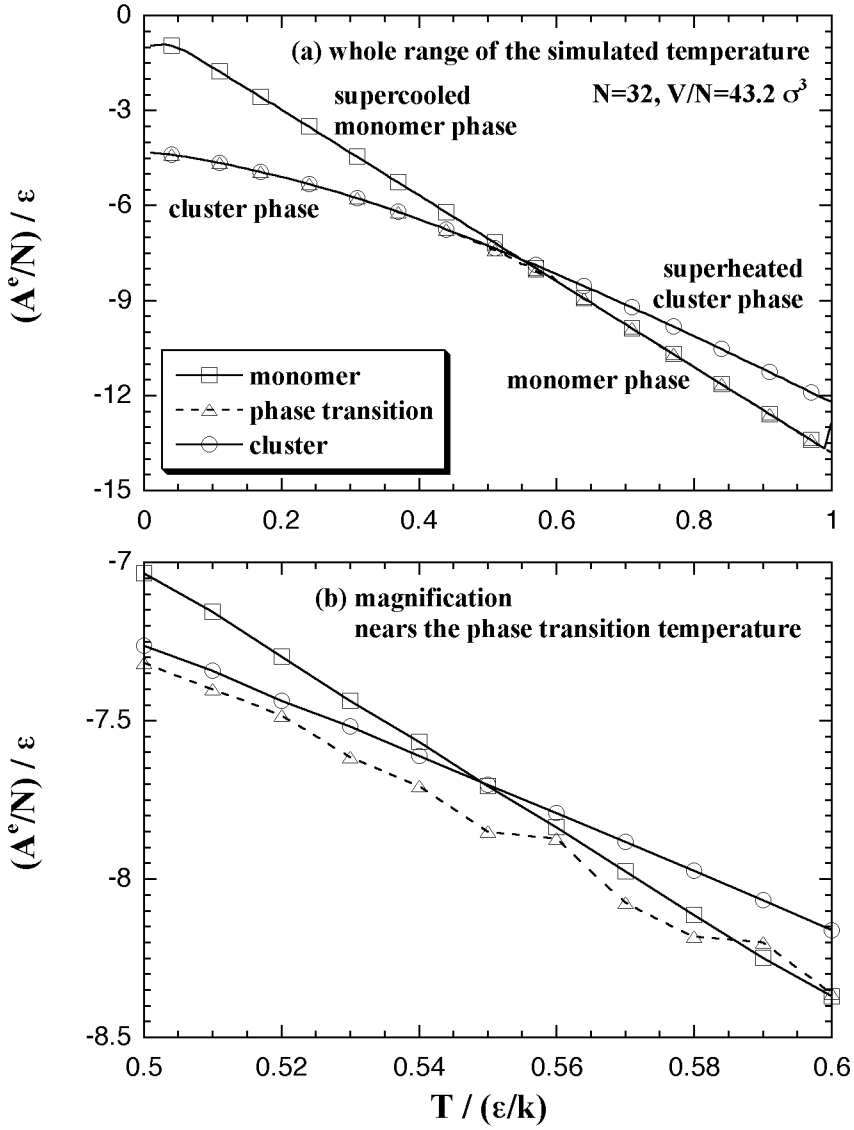

Fig. 3.4. The interaction term of Helmholtz free energy per particle versus temperature plots on 32-particle system. The figure (a) shows the whole range of the simulated temperature, while the figure (b) is a magnification nears the phase transition temperature. The curves of the monomer phase and the cluster phase calculations intersect at $T \approx 0.55\ \varepsilon/k$. The curve of the phase transition calculation disagrees with the curves of the other restricted calculations.

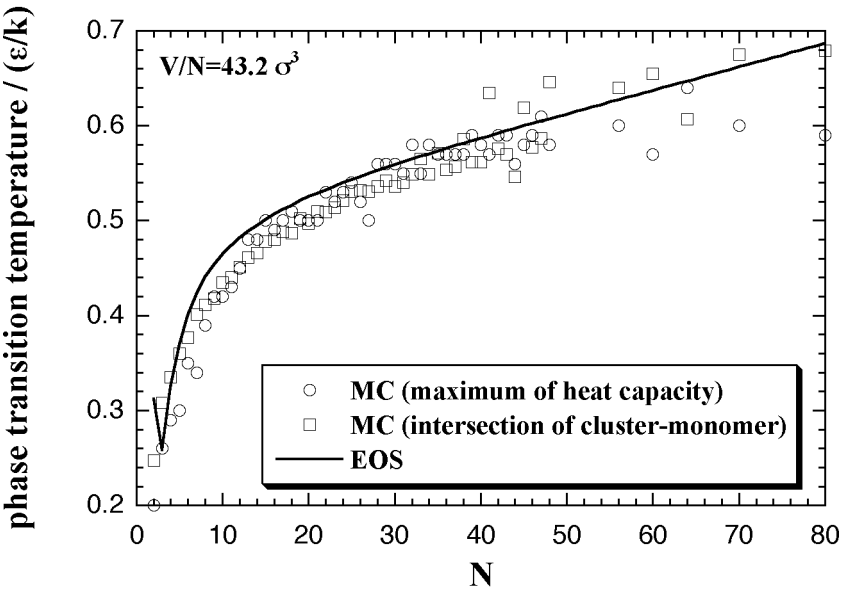

Fig. 3.5. The cluster-monomer phase transition temperature versus the number of particles plots. The circles are obtained from the maximum of the interaction term of heat capacity on each number of particles (like Fig. 3.2a), while the squares are the intersection of the curves of the cluster phase and the monomer phase calculations (like Fig. 3.4). The solid curve shows the phase transition temperature from the intersection of the approximated functions, discussed below.

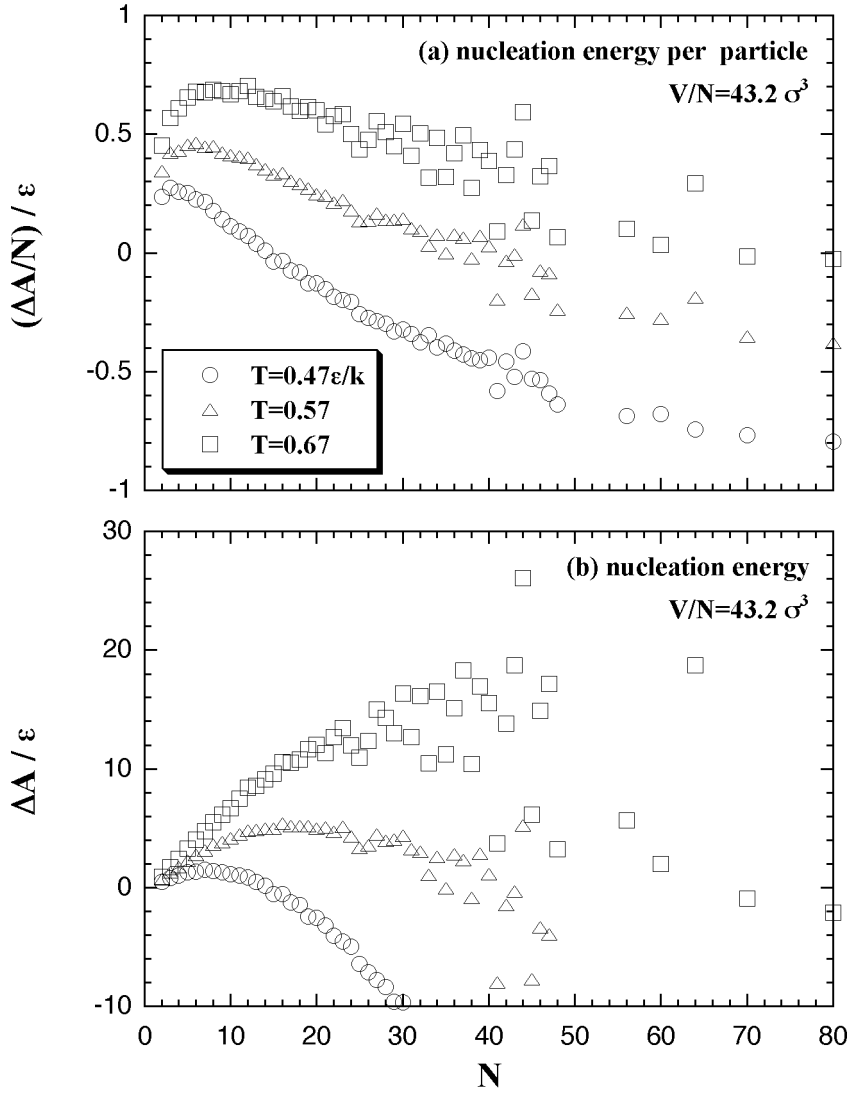

Fig. 3.6. The Helmholtz free energy of the homogeneous nucleation versus the number of particles plots. The values per particle (a) and the values of the system (b) are shown, respectively. It seems that the plots about the *N*-particle system (b) have maxima on each temperature.

3.2. Approximated Functions for the Equation of State

The interaction energy U^e, the interaction entropy S^e, the interaction term of Helmholtz free energy A^e, and the nucleation free energy change ΔA can be described as a function of the number of particles and the temperature. We assumed the approximated functions for development of an equation of state (EOS) of the nucleation free energy. Which are designed as the power series for easy handling:[13,14,III]

$$\frac{U_m^e}{N} = \sum_{i=0}^{2} \left\{ a_i' N^{-i} \right\}, \tag{3.1}$$

$$\frac{S_m^e}{N} = \sum_{i=0}^{2} \left\{ b_i' N^{-i} \right\}, \tag{3.2}$$

$$\frac{U_c^e}{NT} = \sum_m \sum_n \left\{ a_{mn}' N^m T^n \right\}, \tag{3.3}$$

$$(m = -2,-1,0,1; n = -5,-4,-3,-2,-1,0,1)$$

$$\frac{S_c^e}{N} = \sum_p \sum_q \left\{ b_{pq}' N^p T^q \right\}. \tag{3.4}$$

$$(p = -2,-1,0; q = -6,-5,-4,-3,-2,-1,0,1)$$

Here, the subscripts *m* and *c* indicate the monomer phase and the cluster phase, respectively. In the monomer phase calculation, the interaction energy and the interaction entropy have little dependence on the temperature except for the two ends of the simulated temperature, as shown in Fig. 3.1 and 3.3. Then, we assumed the expressions for the monomer phase (eqs. 3.1 and 3.2) to only depend on the number of particles and we used the averaged values at the intermediate temperature for such approximations. The expression for the interaction energy of the cluster phase, eq. 3.3, is assumed as (U_c^e/NT), that aims to accurate the approximation.

The interaction entropy is obtained from the interaction energy by eqs. 2.4-2.8. Therefore, in essential, the function for the interaction energy ought to predict not only the interaction energy but also the interaction entropy, and two approximated functions are sufficient concerning the EOS: for the monomer phase and for the cluster phase. In the case of the monomer phase, we assumed that the interaction energy and the interaction entropy have no dependence on the temperature, then the interaction terms of the heat capacity and the entropy should become zero. Accordingly, the function for the

interaction entropy is described separately from the one for the interaction energy, and we used the equilibrated value of the decomposed monomer phase in the phase transition calculation instead of the value of the monomer phase calculation. On the other hand, the interaction energy and the interaction entropy of the cluster phase were approximated unsuccessfully by the one expression for the interaction energy. It may be caused by the error from the limited number of MC steps and the dispersion of the MC results that is due to the treating of the meta- or unstable phase: the superheated cluster.

The coefficients of the approximated functions, a'_i, b'_i, a'_{mn}, and b'_{pq} are determined by least-squares fittings. The fitting algorithm is the Modified Gram-Schmidt method.[IV] Tables 1 and 2 show the obtained coefficients. When we regard the relative deviation of the thermodynamic property X to be

$$\delta' X \equiv \frac{\left\langle \left[\delta X\right]^2 \right\rangle^{1/2}}{\left\langle X^2 \right\rangle^{1/2}}, \tag{3.5}$$

we obtained the deviations of the each function as $\delta'(U_m^e/N) = 3.57\times10^{-4}$, $\delta'(S_m^e/N) = 6.59\times10^{-5}$, $\delta'(U_c^e/NT) = 0.00315$, and $\delta'(S_c^e/N) = 0.0602$. Figures 3.7-3.10 show the results of the least-squares fittings. In the figures, the circles, triangles, and squares indicate the MC results, and the solid curves are the approximated functions. It can be seen that the functions well reproduce the MC results. The curve of the nucleation free energy, like the Fig. 3.10 (b), has a maximum against the number of particles that corresponds to the values of the critical nucleus. Which, the free energy ΔA^* and the size N_A^*, are shown in Fig. 3.11. Both curves simply increase against the temperature.

As already stated, we assumed the approximated functions separately for the interaction energy and the interaction entropy of the cluster phase. Figure 3.12 shows the comparison between the two functions of the cluster phase; the expression of the interaction entropy (eq. 3.4), and the interaction entropy obtained from the expression of the interaction energy (eq. 3.3) with eqs. 2.5-2.8. Since the two curves roughly agree, we confirmed the consistency of separate treating with the two expressions for the cluster phase.

Table 1. Results of the least-squares fittings for the monomer phase: a'_i and b'_i. The symbol E−1 means 10^{-1}.

i	a'_i	b'_i
0	−2.650E−1	1.547E+1
1	4.057E−1	−4.462E+1
2	−2.316E−1	3.761E+1

Table 2. Results of the least-squares fittings for the cluster phase: a'_{mn} and b'_{pq}.

a'_{mn}		m			
		−2	−1	0	1
	−5	−4.05E−2	2.42E−1	−2.55E+1	5.27E+1
	−4	5.67E−2	4.04E+0	6.61E+0	−3.15E+1
	−3	−3.07E−2	−5.01E+0	1.69E+1	−1.54E+1
n	−2	9.60E−4	7.11E−2	−1.75E−1	6.91E−3
	−1	−3.19E−5	−2.62E−3	8.45E−3	−4.40E−3
	0	4.54E−7	3.96E−5	−1.43E−4	9.86E−5
	1	−2.19E−9	−1.97E−7	7.53E−7	−5.75E−7

b'_{pq}		p		
		−2	−1	0
	−6	5.84E−1	−2.17E+1	4.27E+1
	−5	1.58E+1	−3.30E+1	7.73E+0
	−4	−3.65E+0	1.32E+1	−1.22E+1
	−3	4.38E−1	−1.94E+0	2.14E+0
q	−2	−2.49E−2	1.20E−1	−1.42E−1
	−1	6.88E−4	−3.49E−3	4.23E−3
	0	−8.75E−6	4.55E−5	−5.61E−5
	1	3.95E−8	−2.09E−7	2.60E−7

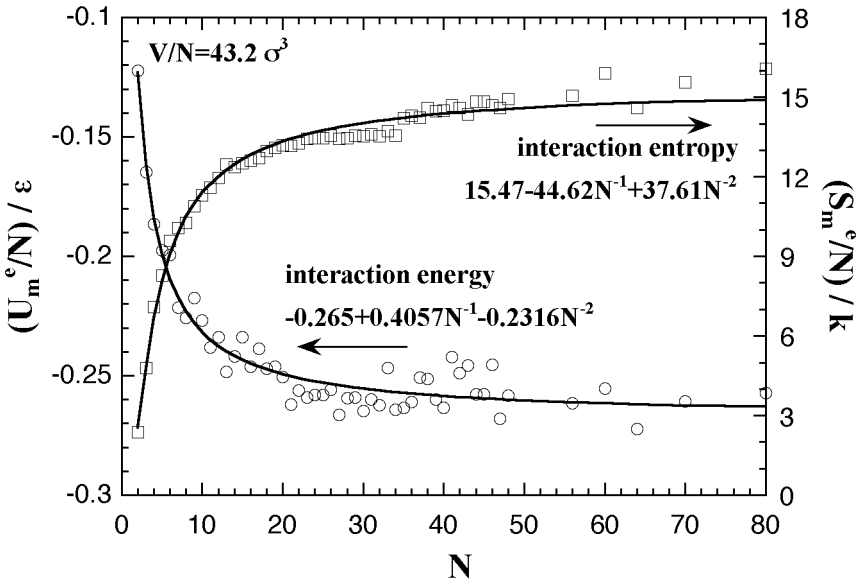

Fig. 3.7. Results of the least-squares fittings of the monomer phase. The circles and squares are the equilibrated values of the decomposed monomer phase at the each number of particles.

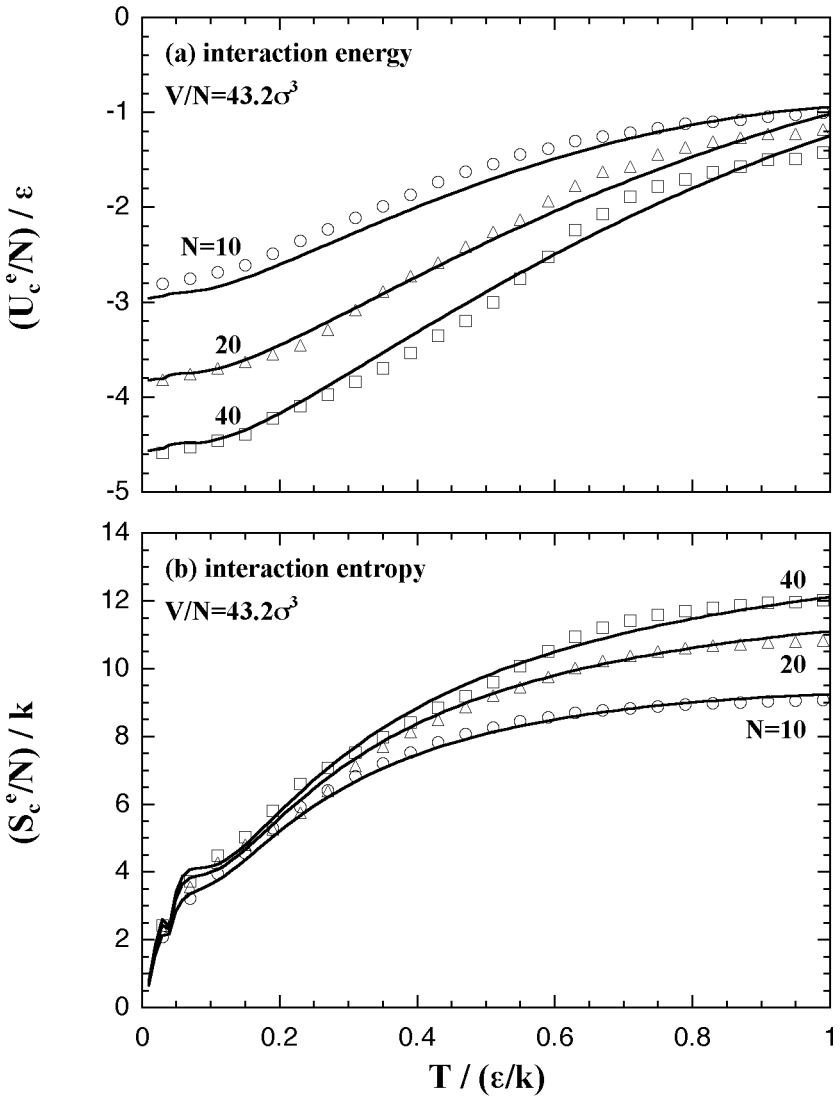

Fig. 3.8. Results of the least-squares fittings of the cluster phase. The interaction energy (a) and the interaction entropy (b) are plotted versus temperature as the values per particle.

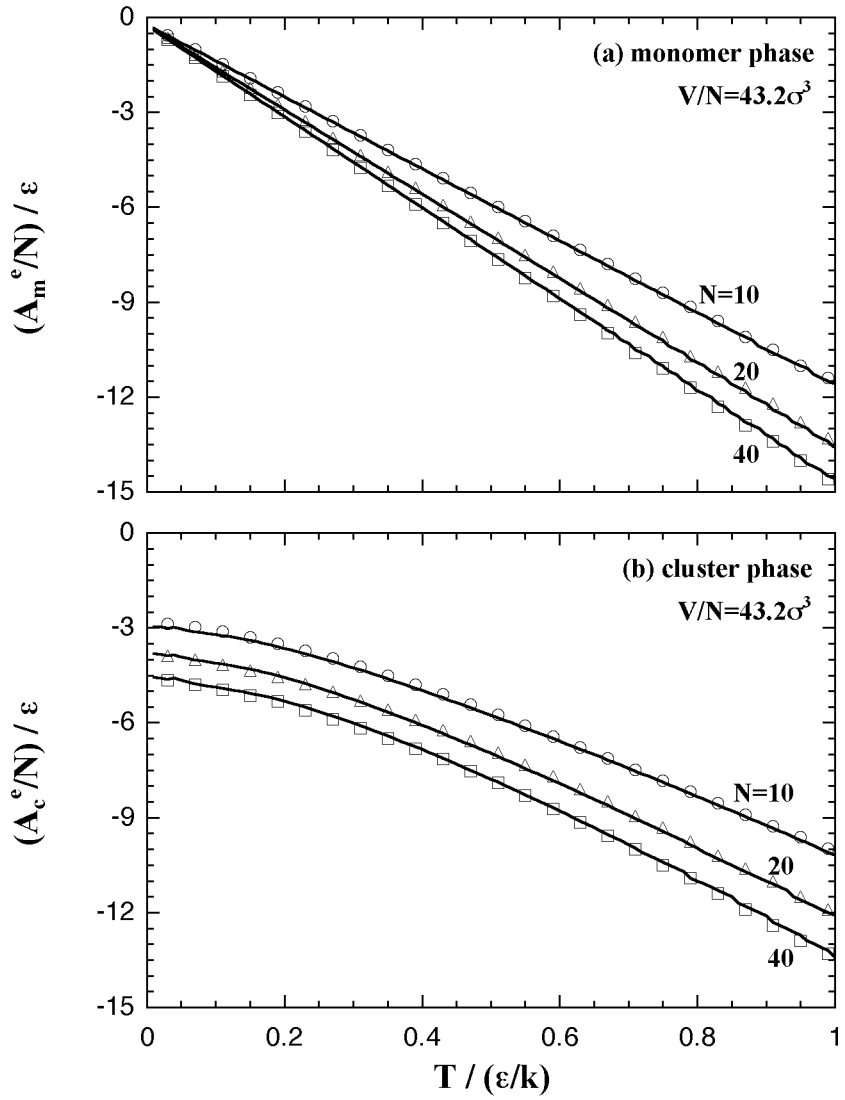

Fig. 3.9. Fitting results of the interaction term of Helmholtz free energy per particle versus temperature plots. The figure (a) shows the results of the monomer phase, and (b) the cluster phase.

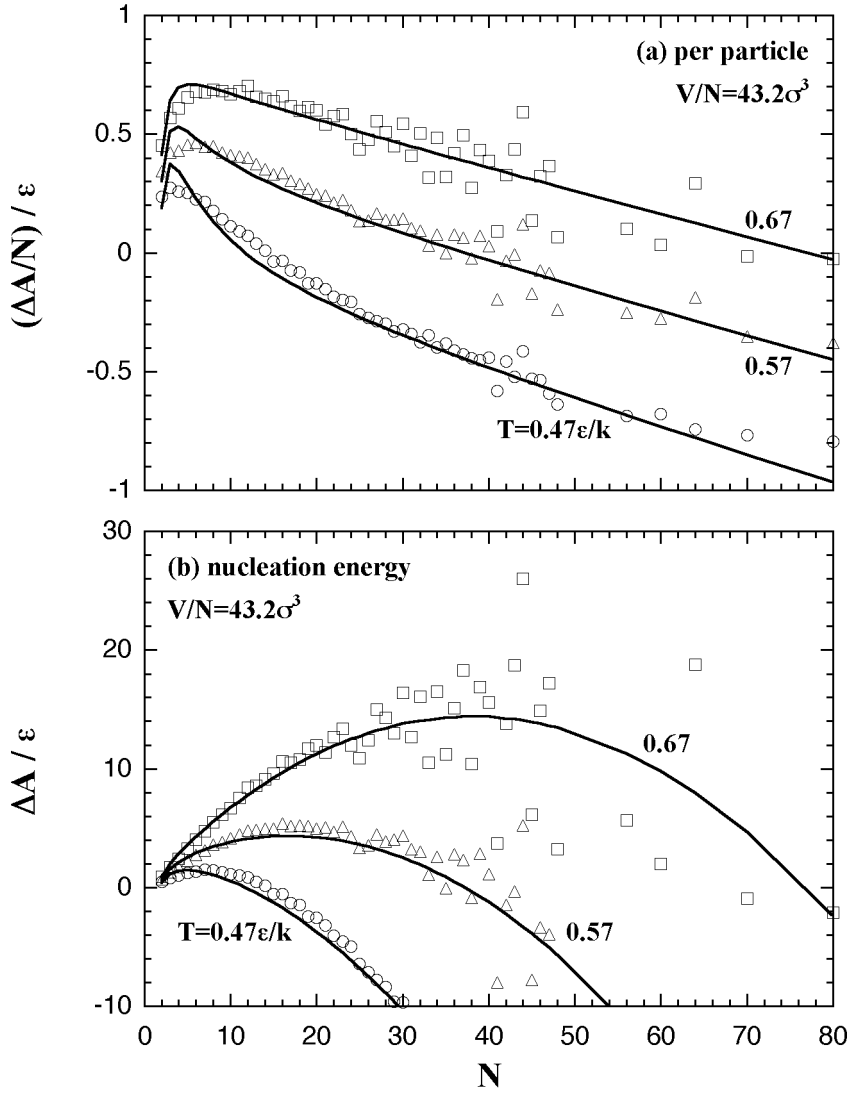

Fig. 3.10. The Helmholtz free energy of the homogeneous nucleation that is obtained as the difference between the free energies of the cluster phase and the monomer phase. The figure (a) shows the values per particle, and (b) the values of the system. In the figure (b), a maximum is observed about ΔA 15 ε at N 40 in the case of the focused temperature: T = 0.67 ε/k.

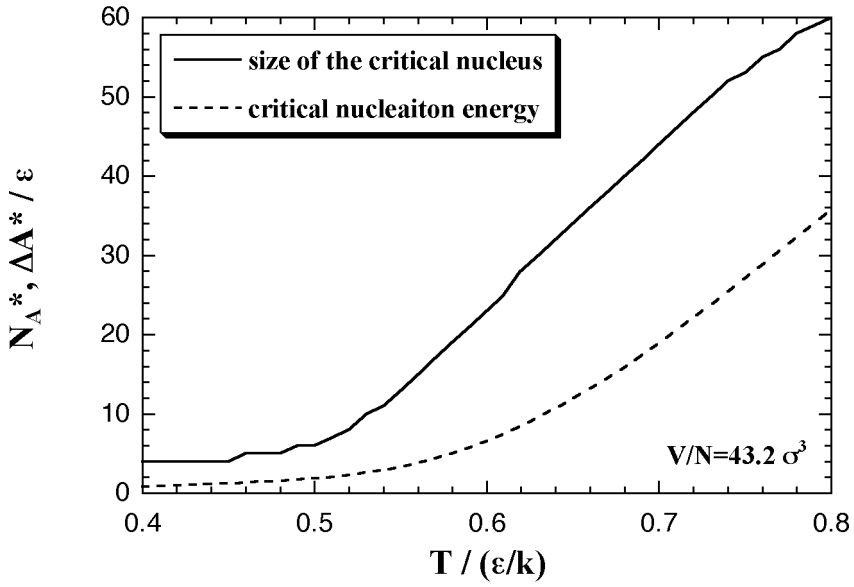

Fig. 3.11. The values of the critical nucleus versus the temperature plots. The solid curve is the size N_A*, and the broken curve is the nucleation energy ΔA*.

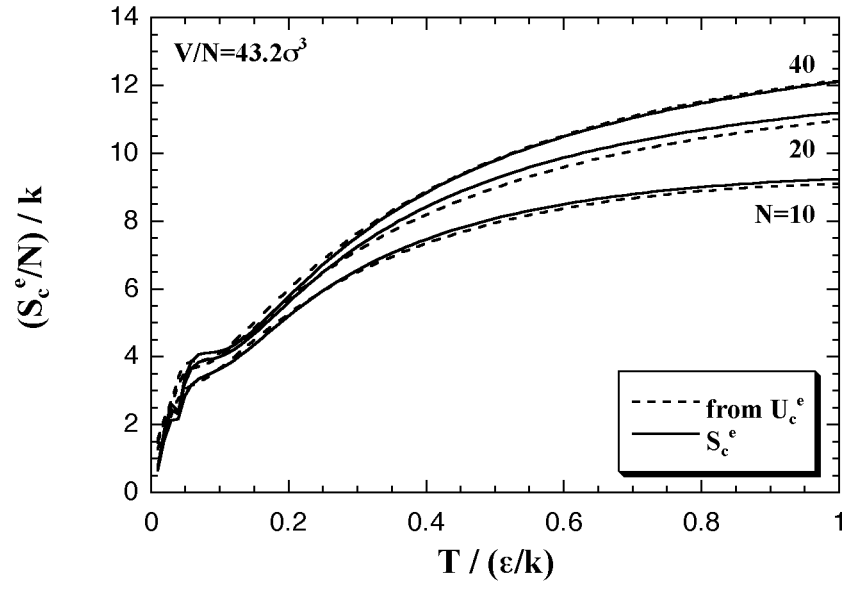

Fig. 3.12. Comparison between the two expressions for the cluster phase. The solid curves show the expression for the interaction entropy, and the broken curves the S_c^e from the expression for the interaction energy.

Chapter 4: MONTE CALRO SIMULATIONS UNDER VARIOUS VOLUMES PER PARTICLE

The secondary MC simulations were performed under various volumes per particle. These simulations aim to assume the volume dependence of the nucleation free energy. The detailed procedure of which is much the same as the fixed-volume per particle simulation in the previous chapters. Here we explain where is different from the fixed-volume simulation in which procedure and the observed results.

We performed the MC simulations with changing number of particles N, temperature T, and volume per particle V/N: as N = 2-80, T = 0.01-1.00 ε/k, and V/N = 30, 43.2, 90, 240, and 1000 σ^3. Figure 4.1 shows the simulated states in the (N,V/N) plane; the number of states is 128. We adopted only the face-centered cubic lattice as an initial lattice of the cluster stabilization process. It is caused that, particularly in the large-N system, the stable cluster is hardly obtained if the simple cubic and the body-centered cubic were chosen as the initial lattice of the first stage (details in Appendix B). At the simulations of V/N = 43.2 σ^3, we confirmed that the interaction energy and the interaction entropy of the monomer phase do not depend on the temperature, and we assumed the equilibrated values after the cluster decomposition in the phase transition calculation into the interaction energy and the interaction entropy of the monomer phase. Therefore, the monomer phase calculation was not performed at the simulations in this chapter.

In the cluster phase calculation, we restricted the configuration of the system to keep a unity cluster still high-temperature with the Stillinger's cluster criterion. However, the criterion focuses only the interparticle distance, so the shape of the cluster is not considered.[5,15] Therefore, if the configuration satisfies only a threshold value of the interparticle distance, 1.5 σ, the configuration is permitted as the cluster phase even though the configuration is collapsed and stretched by heating, like Fig. 4.2. The stretched clusters appear frequently when the number of particle becomes larger or the volume per particle larger. However, we found in our simulations a tendency that the cluster keeps the

spherical shape still the high-temperature on the specific numbers of particles; N = 27, 32, 34 and 64. We surmise that it is similar to the Magic Number of cluster formation: i.e., the specific number of particles that had the inclination to form a rather stable cluster.[16,V] An example of the stable configuration of 64-particle cluster is shown in Fig. 4.3.

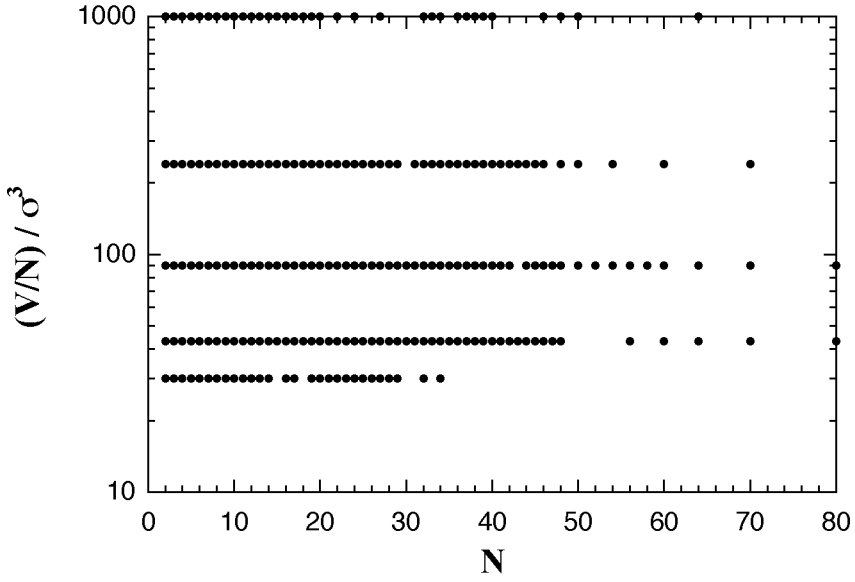

Fig. 4.1. Map of the simulated states in the number of particles versus the volume per particle plane. The number of the states is 128.

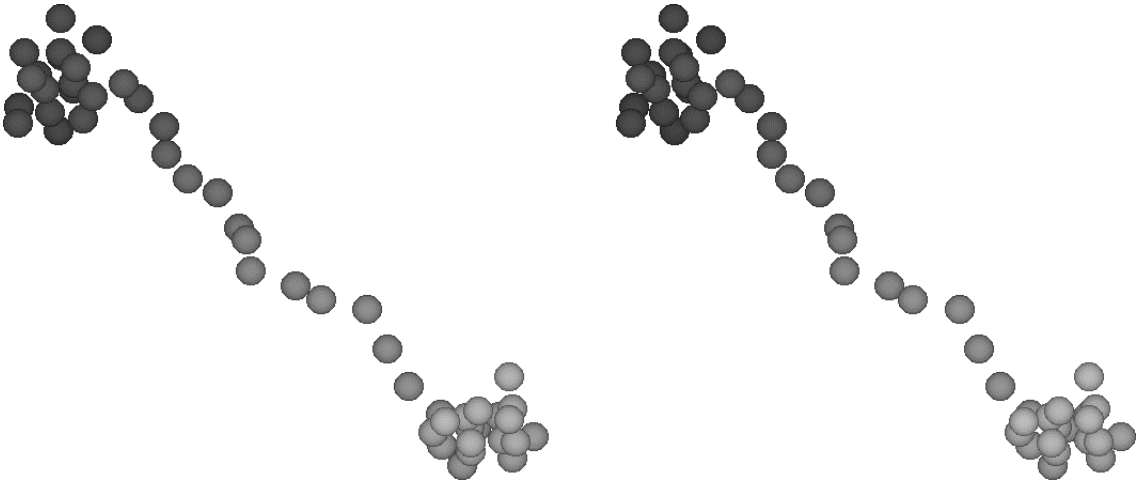

Fig. 4.2. Stereoscopic snapshot of the stretched cluster phase; $N = 50$, $T = 1.00\ \varepsilon/k$ and $V/N = 1000\ \sigma^3$. This configuration satisfies the Stillinger's cluster criterion.

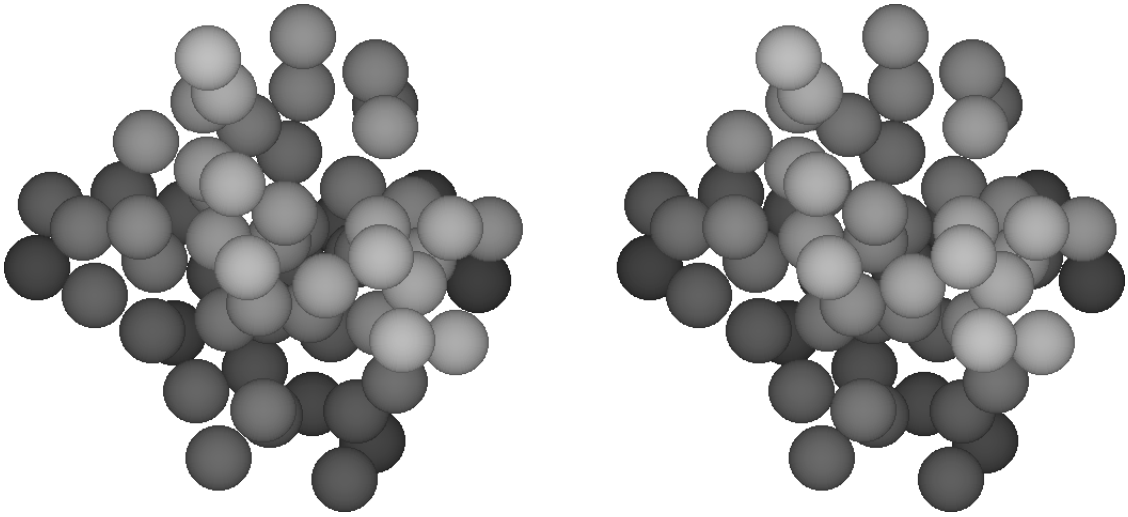

Fig. 4.3. Stereoscopic snapshot of the stable cluster as spherical, $N = 64$, $T = 1.00\ \varepsilon/k$ and $V/N = 90\ \sigma^3$. The 64-particle cluster is stable and keeps the spherical shape considerably irrespective of the temperature and the volume per particle.